Available online at www.sciencedirect.com

ScienceDirect

Procedia Structural Integrity 2 (2016) 903–910

Structural Integrity Procedia

www.elsevier.com/locate/procedia

21st European Conference on Fracture, ECF21, 20-24 June 2016, Catania, Italy

Interpretation of creep crack growth data for $\frac{1}{2}$CMV steel weldments

Muneeb Ejaz[a,*], Catrin M. Davies[a], David W. Dean[b]

[a]*Department of Mechanical Engineering, Imperial College London, South Kensington Campus, London SW7 2AZ, UK*
[b]*EDF Energy Generation Ltd., Barnwood, Gloucester GL4 3RS, UK*

Abstract

$\frac{1}{2}$Cr$\frac{1}{2}$Mo$\frac{1}{4}$V ($\frac{1}{2}$CMV) steel has been used in high temperature power plant piping due to its enhanced weld properties. Creep crack growth testing has been performed on compact tension C(T) specimens of $\frac{1}{2}$CMV (low alloy ferritic) steel at 540 °C on both parent metal specimens as well as fine and coarse grained heat affected zone (HAZ) specimens, where the initial crack is located within the HAZ. The data has been interpreted using the fracture mechanics parameter C^* against the crack growth rate. The creep toughness parameter, K^c_{mat}, is also evaluated for the material. It was seen that, for a given C^* value, the fine grained HAZ material generally exhibits higher crack growth rates than the post weld heat treated coarse grained HAZ.

Peer-review under responsibility of the Scientific Committee of ECF21.

Keywords: creep crack growth; $\frac{1}{2}$CMV; K^c_{mat}; Weldments; Heat affected zone (HAZ)

1. Introduction

$\frac{1}{2}$Cr$\frac{1}{2}$Mo$\frac{1}{4}$V ($\frac{1}{2}$CMV) low alloy steel has been widely used in steam piping for convention power stations, particularly in the UK. With aging plants becoming an ever increasing issue, it is important that the failure mechanisms in the power-plant components are understood and can be predicted. Creep failure mechanisms are predominant in high temperature plant components, and with a number of the components defected, it is important that the creep crack initiation (CCI) and growth (CCG) behaviour of these components are characterised. Intergranular creep cracks are often formed in the heat affected zone (HAZ) of welded joints in $\frac{1}{2}$CMV, hence it is vital that the CCG behaviour of the HAZ in addition to parent materials be determined.

In this work, CCG data from the $\frac{1}{2}$CMV parent and HAZ programmes at EDF Energy (Baker and Gladwin, 2004) have been analysed. Data was obtained from tests carried out on compact tension C(T) specimens at 540 °C. The method of analysis and validation follows that outlined in ASTM E 1457 (ASTM, 2015). The suitability of the, C^*, parameter to characterise CCG rates is assessed. In addition, due to the increased recognition of the time dependent failure assessment diagram (TDFAD) approach for the prediction of CCI (BEGL, 2003), the creep toughness parameter, K^c_{mat}, has been evaluated at given crack extensions of 0.2 and 0.5 mm.

* Muneeb Ejaz.
E-mail address: muneeb.ejaz09@imperial.ac.uk

Peer review under responsibility of the Scientific Committee of ECF21.
10.1016/j.prostr.2016.06.116

Nomenclature

β	constant in K^c_{mat} relationship with time
Δ	load-line displacement
Δ_e	elastic load-line displacement
Δ_p	plastic load line displacement
Δ_c	creep load line displacement
$\dot{\Delta}$	load line displacement rate
$\dot{\Delta}_c$	creep load line displacement rate
$\dot{\Delta}_i$	instantaneous load-line displacement rate associated with elastic and plastic strains
$\dot{\Delta}_{i,e}$	instantaneous load-line displacement rate associated with elastic strains
Δa	amount of crack growth
η	geometric factor to calculate C^* from load line displacement rate
ν	Poisson's ratio
σ	equivalent stress
$\sigma_{0.2}$	0.2% proof stress
ϕ	exponent in $\dot{a}$ correlation with C^*
ψ	power-law exponent in K^c_{mat} relationship with time
a	crack length
a_0	initial crack length measurement
a_f	final crack length measurement
$\dot{a}$	crack growth rate
n	power-law creep stress exponent
t_T	transition time
t_f	test duration
A	coefficient in the power-law creep strain rate equation
A_p	plastic area under the load-line displacement curve
B	specimen thickness
B_n	specimen net thickness between side-grooves
C^*	steady-state creep fracture mechanics parameter
D	material constant in $\dot{a}$ correlation with C^*
E	elastic Young's modulus
E'	effective elastic modulus = $E/(1-\nu^2)$ for plane strain
H	factor to calculate C^* from load-line displacement rate = $n/(n+1)$ for a C(T) specimen
H'	factor to calculate K^c_{mat} = 1 for a C(T) specimen
K^c_{mat}	creep fracture toughness parameter
P	applied load
W	specimen width

1.1. Background to creep fracture analysis

The equivalent creep strain rate, $\dot{\varepsilon}_c$, in power law creeping materials can be described in terms of the equivalent stress, σ, by

$$\dot{\varepsilon}_c = A\sigma^n \tag{1}$$

where n and A represent the power-law creep exponent and coefficient, respectively.

The CCG rate, $\dot{a}$, can be uniquely described by $C^*$when steady-state conditions prevail (Webster and Ainsworth, 2013),

$$\dot{a} = DC^{*\phi} \tag{2}$$

where D and ϕ are material constants which may be temperature and stress state dependent. Typically ϕ is found to be close to unity.

2. Materials

Segments of normalised and tempered $\frac{1}{2}$CMV pipes of 350 mm outer diameter and 65 mm wall thickness were used to fabricate a weldment, joined by $2\frac{1}{4}$Cr1Mo weld metal. Coarse and refined HAZ microstructures were separately produced on opposite sides of the weld by predetermined weld bead deposition. The circumferential butt weld faces were perpendicular to the pipe axis and the weld was wide enough to allow the extraction of a specimen from the HAZ on both sides of the weld (Baker and Gladwin, 2004). Indicative material properties for $\frac{1}{2}$CMV parent material at 540 °C are shown in Table 1.

Table 1. Indicative material properties for $\frac{1}{2}$CMV parent material at 540 °C.

Property	Value
E	169 GPa
$\sigma_{0.2}$	235 MPa
n	4

3. Experimental procedure

3.1. Test specimen details

Specimen blanks were extracted from the normalised and tempered $\frac{1}{2}$CMV parent material in the pipe axial-radial orientation and the coarse and refined HAZ regions in the weld transverse-radial orientation. C(T) specimens of thickness (B) 25 mm were machined according to ASTM E-399 (ASTM, 2013). However, due to the reduced thickness in the weld region, the width (W) of some specimens had to be reduced to 47 mm instead of the standard 50 mm. Prior to testing, the specimens were fatigue pre-cracked at room temperature in accordance with the ESIS Procedure (ESIS P1-92, 1992) and then side grooved on each side by 10% of their thickness using a Charpy V-notch profile cutter. The specimen dimensions are described in Table 2. The notations P, F and C in the specimen names denote parent, fine grain and corase grain, respectively.

Table 2. Specimen geometry details (P ≡ parent, F ≡ fine grain, C ≡ coarse grain)

Specimen name	W (mm)	B (mm)	B_n (mm)	a_0 (mm)	a_0/W
C(T)P1	47.00	24.86	19.80	24.43	0.52
C(T)P2	47.00	24.87	20.23	24.20	0.51
C(T)F1	47.09	24.83	19.92	23.34	0.50
C(T)F2	47.03	24.84	19.95	23.06	0.49
C(2)C1	47.00	24.82	19.98	24.16	0.51

3.2. Testing Details

CCG tests were performed in over-slung lever arm constant load tensile creep machines at EDF Energy. The testing procedure is described in detail in (Gladwin, 2000) and the method of analysis and data validation follows that found in ASTM E-1457 (ASTM, 2015). All tests were carried out at a temperature of 540 °C. The testing details are summarised in Table 3.

Table 3. Specimen test details (P ≡ parent, F ≡ fine grain, C ≡ coarse grain)

Specimen name	Load, P (N)	Test duration, t_f (h)	a_f/W	$a_f - a_0$ (mm)	t_T/t_f (%)	$t_{0.2}/t_f$ (%)
C(T)P1	16,000	1006.52	0.56	1.85	14.55	36.56
C(T)P2	19,000	413.06	0.96	20.95	13.58	4.23
C(T)F1	15,000	118.87	0.55	2.66	35.12	1.04
C(T)F2	8750	722.90	0.64	7.05	26.97	6.84
C(2)C1	17,000	46.85	0.65	6.33	26.55	2.67

4. Analysis of creep crack growth data

The procedures outlined in ASTM E 1457 (ASTM, 2015) have been incorporated here for the experimental determination of the C^* parameter for C(T) geometries. In addition, the creep toughness parameter K^c_{mat}, will be determined. The methods are summarised here as follows.

4.1. Determination of experimental C^* formula

The steady-state crack growth parameter C^* is determined directly from the creep load line displacement rate, $\dot{\Delta}_c$, as

$$C^* = \frac{P\dot{\Delta}_c}{B_n(W-a)}H\eta \tag{3}$$

where P is the applied load and H and η are geometric functions. The function H for a C(T) geometry is given by $H = n/(n+1)$ where n is the creep power-law stress exponent. The mean value of η is taken as 2.2, consistent with the numerical analysis done on C(T) specimens and reported in (Davies et al., 2006).

The experimentally determined load line displacement rate, $\dot{\Delta}$, may be subdivided into an instantaneous component, $\dot{\Delta}_i$, and a time-dependent component, $\dot{\Delta}_c$, that is related to the accumulation of creep strains as

$$\dot{\Delta}_c = \dot{\Delta} - \dot{\Delta}_i \tag{4}$$

The instantaneous displacement rate, $\dot{\Delta}_i$, can be further divided into elastic and plastic components. The elastic instantaneous creep component, $\dot{\Delta}_{i,e}$, is defined as

$$\dot{\Delta}_{i,e} = \frac{2\dot{a}B_n}{K}\frac{K^2}{E'} \tag{5}$$

where B_n is the net specimen thickness between the side grooves and E' is the effective modulus $[E/(1-\nu^2)$ for plane strain and E for plane stress]. All analyses carried out in this work assume plane strain conditions and the instantaneous plastic displacement rate is considered negligible (i.e. the creep and plastic displacement rates have not been treated separately).

4.2. Validity criteria for the use of C^*

To ensure that steady-state creep processes have developed, ASTM E 1457 (ASTM, 2015) specifies that C^* may be used as the relevant parameter provided the following three criteria are satisfied:

1. The transition time, t_T, must be exceeded (Riedel and Rice, 1980). Under the assumption of plane strain and elastic or small scale yielding conditions, the transition time is taken as the maximum value estimated from the crack growth test as

$$t_T = \max\left[\frac{K^2(1-\nu^2)}{E(n+1)C^*}\right] \tag{6}$$

   where K is the stress intensity factor. It represents the time required for extensive creep conditions to develop i.e. the time required for the creep process zone ahead of the crack tip to engulf a considerable portion of the uncracked ligament.
2. The material must be established as being creep-ductile i.e. the creep load line displacement rate, calculated from Equation 4, constitutes at least half of the total load line displacement rate: $\dot{\Delta}_c/\dot{\Delta} \geq 0.5$.
3. For data points to be valid $\Delta a \geq 0.2$ mm. CCG data obtained prior to a crack extension of 0.2 mm is considered to be in a transient region where damage ahead of the crack-tip has not reached a steady-state.

4.3. Evaluation of the creep toughness parameter, K^c_{mat}

Alternative methods for determining the time required for a given crack extension to occur are included in the EDF Energy R5 procedure (BEGL, 2003). These have been used to predict creep crack initiation (Davies et al., 2003; Baker et al., 2003). The methods incorporate the use of a high temperature time dependent failure assessment diagram (TDFAD) which requires the evaluation of a time dependent creep toughness parameter, K^c_{mat}. For a C(T) specimen, this can be determined from

$$K^c_{mat} = \sqrt{K^2 + \frac{\eta E'}{B_n(W-a)}[H' A_p + HP\Delta_c]} \tag{7}$$

where $H' = 1$ for a C(T) specimen. In Equation 7, A_p represents the area under the load displacement curve associated with plasticity.

It is expected that K^c_{mat} follows the power-law relation

$$K^c_{mat} = \beta t^{-\psi} \tag{8}$$

where β is the correlating coefficient and, ψ is the power-law exponent; typically $\psi = 1/2n$ (Davies, 2009).

5. Results and Discussion

Experimental crack length data normalised by specimen width (a/W) are plotted against test time normalised by test duration (t/t_f) in Figure 1. The parent material specimens are represented by the square symbols, and the fine and coarse grain HAZ specimens are represented by the triangular and circular symbols, respectively. Minimal crack growth is seen prior to 80% of the test duration followed by accelerated crack growth until failure. This points to the significance of creep crack initiation before final failure.

Creep load line displacement, Δ_c, data are plotted against normalised time in Figure 2. For clarity, the maximum value shown in Figure 2 is 0.5 mm, although the maximum creep load line displacement for specimen C(T)C1 was found to be 3.15 mm. Characteristic to each curve shown is a period of stress relaxation due to creep, where the displacement rate is seen to decrease, followed by a linear region of constant displacement rate. In the final region, the displacement rate is seen to rapidly increase until failure.

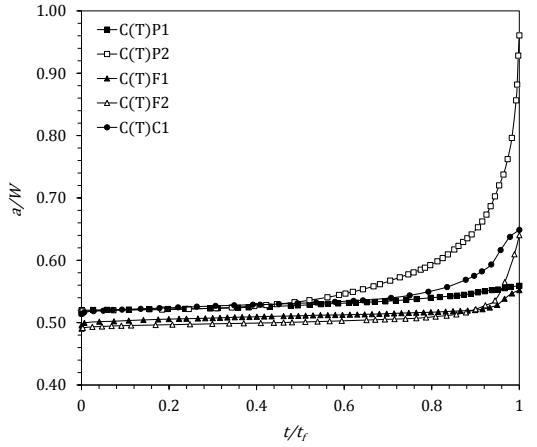

Fig. 1. Normalised crack length with normalised time.

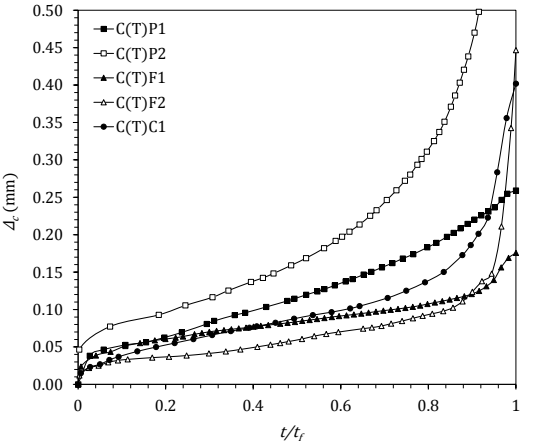

Fig. 2. Creep load line displacement, Δ_c,with normalised time

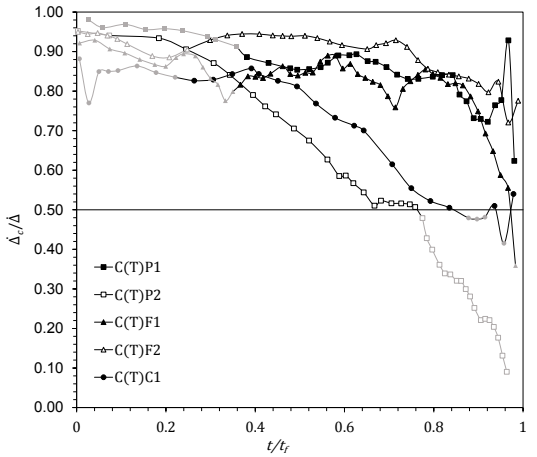

Fig. 3. Analysis of validity criteria for the correlation of $\dot{a}$ with C^*.

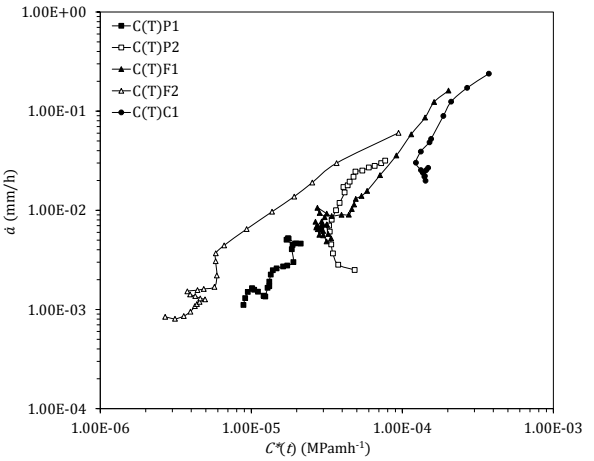

Fig. 4. Creep load line displacement, Δ_c,with normalised time

5.1. Characterisation of CCG

The validity criterion for the use of the C^* parameter is assessed in Figure 3 where the ratio $\dot{\Delta}_c/\dot{\Delta}$, obtained from equations 4 and 5, is plotted against normalised time. The invalid points, for which $\Delta a < 0.2$ mm and $\dot{\Delta}_c/\dot{\Delta} > 0.5$, are shaded in grey. As shown in Table 3, the time for 0.2 mm crack growth is less than the transition time for all specimens except C(T)P1. Hence, the time required for extensive steady-state creep conditions to develop is further enforced, and data points for which $t < t_T$ are also shaded grey. The higher crack growth rate associated with specimen C(T)P2 explains the lower creep to load line displacement ratio, and nearing the end of the test $\dot{\Delta}_c/\dot{\Delta} < 0.25$ indicating creep-brittle fracture. It can be concluded from the analysis of validity that the majority of the data fall within the creep-ductile regime, where $\dot{\Delta}_c/\dot{\Delta} \geq 0.5$, and hence C^* may be used as the characterising parameter (ASTM, 2015).

Figure 4 shows the correlation of CCG rates with C^* for all the valid data points shown in Figure 3. It may be seen that the crack growth data from all specimens show a linear correlation between $\dot{a}$ and C^*, falling within the same scatter band. The measured CCG rate in the HAZ specimens is generally higher than that in the homogeneous parent material. It can be further seen that, for a given C^* value, the two fine grain HAZ specimens, C(T)F1 and C(T)F2, generally exhibit higher crack growth rates than the coarse grain HAZ specimen, C(T)C1.

A regression line was fitted separately to the data in Figure 4 in order to deduce the constants in Equation 2. The values of D and ϕ were found to be 687.52 and 1.09, respectively. The value of ϕ is above unity and is seen to

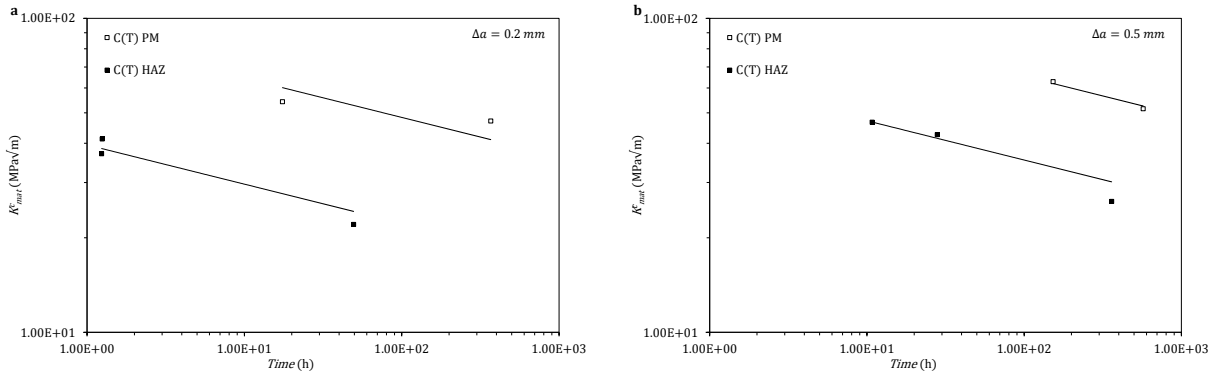

Fig. 5. Comparison of the K^c_{mat} parameter for HAZ and parent material (PM) specimens for a crack extension of (a) 0.2 mm and (b) 0.5 mm.

digress from $n/(n+1)$. This disparity is apparent from the 'tails' seen in the crack growth data of all specimens in Figure 4. These 'tails' are attributed to a combination of stress redistribution and primary creep i.e. damage building up to a steady-state (Webster and Ainsworth, 2013). Although all data points are valid (i.e. global creep steady-state conditions have developed), some data points from the 'tails' are still present and crack growth is seen to be well-established at a later stage where all data points have superimposed onto a single line. Standard procedure suggests that the tails are generally removed after 0.2 mm crack extension and to omit the tails when fitting the regression line so that the scatter may be reduced and a ϕ value closer to unity obtained (ASTM, 2015). Nevertheless, to remain conservative, the regression line has been fitted to all valid data inclusive of the tails.

5.2. Creep toughness, K^c_{mat}

The K^c_{mat} values for $\Delta a = 0.2$ and 0.5 mm crack extensions have been calculated from Equation 7 for all specimens and are illustrated in Figure 5(a) and (b), respectively. A regression fit has been made to the data to deduce the values of β and ψ in Equation 8. This best line fit has been made assuming a slope of $\psi = 1/2n$ as specified in (Davies, 2009). It can be seen that this gives sensible fits, specifically for the parent material (PM), which comprises of two data sets. It is seen that the creep toughness of the HAZ specimens is about half of the parent specimens and that a general reduction in K^c_{mat} is observed.

6. Conclusions

Crack growth data from $\frac{1}{2}$CMV parent steel and weldments at a temperature of 540 °C have been examined. Weldments of both fine grain and coarse grain HAZ were analyzed. The procedures outlined in ASTM E1457 have been used in the analysis of crack growth rates attained from C(T) specimens. The valid data points indicate creep-ductile behaviour and good correlation with the C* parameter for both parent material and weld specimens. However, due to the 'tails' apparent in the valid data set, a ϕ value corresponding to $n/n+1$ and below unity was not obtained. The crack growth rates measured in the HAZ specimens were generally higher than those of the parent specimens. The fine grain HAZ specimens were seen to exhibit lower crack growth rates than the coarse grain HAZ specimen. It was also seen that the creep toughness parameter K^c_{mat} decreases for the range of test durations and is lower for the HAZ material than the parent material. Further work is required to obtain creep ductility data to see how the CCG rates and initiation times compare with the NSW models.

Acknowledgements

The authors would like to acknowledge the contributions of Louise Allport of EDF Energy Generation Ltd. and Keith Tanowski of Imperial College London, towards the preparation and analysis of experimental data. This paper is published with permission of EDF Energy Generation Ltd.

References

ASTM, 2013. Standard Test Method for Linear-Elastic Plane-Strain Fracture Toughness KIc of Metallic Materials , 1–33doi:10.1520/E0399-12E03.2.

ASTM, 2015. Standard Test Method for Measurement of Creep Crack Growth Times in Metals. doi:10.1520/E1457-07E04.2.

Baker, A., Gladwin, D.N., 2004. Internal Report: AGR Power Stations Status Report on the 2.25Cr1Mo Weld Metal , 0.5CMV Parent and 0.5CMV HAZ Test Programmes. Technical Report. Britsh Energy.

Baker, A.J., O'Donnell, M.P., Dean, D.W., 2003. Use of the R5 Volume 4/5 procedures to assess creep-fatigue crack growth in a 316L(N) cracked plate at 650 Â°C. International Journal of Pressure Vessels and Piping 80, 481–488. doi:10.1016/S0308-0161(03)00102-9.

BEGL, 2003. An Assessment Procedure for the High Temperature Response of Structures. Technical Report. British Energy Generation Ltd.. Gloucester, UK.

Davies, C.M., 2009. Predicting creep crack initiation in austenitic and ferritic steels using the creep toughness parameter and time-dependent failure assessment diagram. Fatigue and Fracture of Engineering Materials and Structures 32, 820–836. doi:10.1111/j.1460-2695.2009.01388.x.

Davies, C.M., Kourmpetis, M., O'Dowd, N.P., Nikbin, K.M., 2006. Experimental Evaluation of the J or C*. Journal of ASTM International 3, 13221. doi:10.1520/JAI13221.

Davies, C.M., O'Dowd, N.P., Dean, D.W., Nikbin, K.M., Ainsworth, R.A., 2003. Failure assessment diagram analysis of creep crack initiation in 316H stainless steel. International Journal of Pressure Vessels and Piping 80, 541–551. doi:10.1016/S0308-0161(03)00107-8.

ESIS P1-92, 1992. Reccomendations for Determining the Fracture Resistance of Ductile Materials. Technical Report. European Structural Integrity Society. Delft.

Gladwin, D.N., 2000. Internal Report: Creep Crack Growth and Creep Toughness Data for an Austenitic Type 316H Steel. Technical Report. British Energy.

Riedel, H., Rice, J., 1980. Tensile cracks in creeping solids. Fracture Mechanics: 12th Conference , 112–130.

Webster, G., Ainsworth, R.A., 2013. High temperature component life assessment. Springer Science & Business Media.